

Dalton Transactions

Accepted Manuscript



This is an *Accepted Manuscript*, which has been through the Royal Society of Chemistry peer review process and has been accepted for publication.

Accepted Manuscripts are published online shortly after acceptance, before technical editing, formatting and proof reading. Using this free service, authors can make their results available to the community, in citable form, before we publish the edited article. We will replace this *Accepted Manuscript* with the edited and formatted *Advance Article* as soon as it is available.

You can find more information about *Accepted Manuscripts* in the [Information for Authors](#).

Please note that technical editing may introduce minor changes to the text and/or graphics, which may alter content. The journal's standard [Terms & Conditions](#) and the [Ethical guidelines](#) still apply. In no event shall the Royal Society of Chemistry be held responsible for any errors or omissions in this *Accepted Manuscript* or any consequences arising from the use of any information it contains.

Co-molten solvothermal method for synthesizing chalcopyrite $\text{CuFe}_{1-x}\text{Cr}_x\text{S}_2$ ($x \leq$ **0.4): high photocatalytic activity for nitrate ions reduction**

Jia Yang,^a Mufei Yue,^a Jing, Ju,^b Rihong Cong,^a Wenliang Gao,^{a} Tao Yang^{a*}*

^a College of Chemistry and Chemical Engineering, Chongqing University, Chongqing, 400044,

People's Republic of China

^b College of Chemistry and Molecular Engineering, Peking University, Beijing 100871, People's

Republic of China

*Corresponding author, Email: taoyang@cqu.edu.cn; gaowl@cqu.edu.cn, Tel: +86-23-65105065.

Abstract

In literature, it is very difficult to obtain sulfides with Cr^{3+} in tetrahedral coordination. Here, a thiourea-oxalic acid co-molten solvothermal method was applied to synthesize chalcopyrite $\text{CuFe}_{1-x}\text{Cr}_x\text{S}_2$ ($x \leq 0.4$) solid solutions. We propose that oxalic acid plays an important role in the crystallization process of $\text{CuFe}_{1-x}\text{Cr}_x\text{S}_2$ and can greatly restrain the formation of other undesired impurities. The successful incorporation of Cr^{3+} was proved by powder XRD, SEM and EDX mapping (2D elemental distribution). The UV-Vis reflectance spectra of $\text{CuFe}_{1-x}\text{Cr}_x\text{S}_2$ suggest the bandgap energies decrease from 0.80 to 0.61 eV along with the increase of the Cr^{3+} concentration. All $\text{CuFe}_{1-x}\text{Cr}_x\text{S}_2$ ($0 \leq x \leq 0.4$) samples show much higher photocatalytic activities than P25 towards the reduction of nitrate ions in aqueous solution. We speculate that the thiourea-oxalic acid co-molten method may be not only effective to synthesize Fe^{3+} - Cr^{3+} sulfides, but also helpful to incorporate Cr^{3+} to other sulfide systems with MS_4 tetrahedra.

Introduction

Chalcopyrite CuFeS_2 is a well-known material with important optical, electrical and magnetic properties.¹⁻³ It has a tetragonal structure in the space group $I-42d$ ($a \sim 5.3$, $c \sim 10.4$ Å). In fact, it can be considered as a cationic ordered double-sphalerite structure (see Fig. 1). A number of I–III–VI₂ compounds crystallize in the chalcopyrite structure, i.e. AgInS_2 , CuInS_2 and CuGaS_2 , whose band gap energies are in the range of 0.5–2.5 eV, and thus are photon-responsive materials in the utilization of solar energy.⁴⁻⁶ Cr^{3+} has a very similar effective cationic radius with Fe^{3+} , but to the best of our knowledge, it is very difficult to substituted into a chalcopyrite sulfide, because Cr^{3+} is difficult to be situated in a tetrahedral environment constructed by S^{2-} . For example, CuCrS_2 crystallizes in an $R3m$ structure, where Cr^{3+} has an octahedral coordination with S^{2-} .⁷ There was only one exception, $\text{CuGa}_{0.98}\text{Cr}_{0.02}\text{S}_2$ chalcopyrite, reported very recently. Once 2 atom% Cr^{3+} was incorporated, this compound became a wide-spectrum solar absorption material due to an intermediate-band mechanism.⁸ Anyway, it is still challenging to dope Cr^{3+} into a chalcopyrite sulfide with a high concentration.

Usually, chalcopyrite CuFeS_2 can be prepared using solid state reaction or hydrothermal method. In the former case, CuFeS_2 powder is obtained via a direct reaction of the elements or metal sulfides, which requires a high reaction temperature (600–1000 °C) with an inert gas flow.^{9,10} The resultant product usually has a high crystallinity but a low specific surface, which is unfavourable for heterogeneous catalysts. Hydrothermal or solvothermal reaction is relatively promising, indicated by a low reaction temperature, and a uniform particle size. However, hydrothermal method also has the disadvantage of easily forming unwanted phases, such as CuS , Fe_2O_3 , etc., which may deteriorate the purity of the CuFeS_2 powders as well as the photocatalytic activities.¹¹⁻¹³

Synthesizing solid solutions of photocatalysts can not only modulate the potential edges of valence band (VB) or conduction band (CB) but also facilitate the transport of photo-generated e^- and h^+ . Here, quaternary $\text{CuFe}_{1-x}\text{Cr}_x\text{S}_2$ solid solutions ($x \leq 0.4$) were synthesized via a soft-chemistry method. Thiourea and oxalic acid are introduced into a closed system at a relatively low temperature (230 °C) to act as reactants and solvent medium. Side reactions between individual Cu^+ , Fe^{3+} or Cr^{3+} with S^{2-} are generally prohibited, while the simultaneous reaction of all three cations with thiourea can be instructed by the presence of oxalic acid, leading to $\text{CuFe}_{1-x}\text{Cr}_x\text{S}_2$. The successful Cr^{3+} -to- Fe^{3+} doping was proved by XRD, SEM, TEM and EDS, and the upper limit of doping is about 40 atom%. At such a high concentration of Cr^{3+} in chalcopyrite, Cr^{3+} was forced to locate in the tetrahedral coordination of S^{2-} , which may be induced by our new synthetic strategy. In addition, the photocatalytic abilities for the nitrate reduction in aqueous solution were investigated for $\text{CuFe}_{1-x}\text{Cr}_x\text{S}_2$ solid solutions, and it is observed that the Cr^{3+} incorporation into chalcopyrite could significantly enhanced the activity by comparing to the parent compound CuFeS_2 and all are much higher than P25 (nanosized TiO_2).

Experimental section

Synthesis

Typically, stoichiometric $\text{CuCl}_2 \cdot 2\text{H}_2\text{O}$ (0.01 mol), $\text{FeCl}_3 \cdot 6\text{H}_2\text{O}$ and $\text{CrCl}_3 \cdot 6\text{H}_2\text{O}$ were mixed evenly with oxalic acid (1.50 g) and excessive thiourea (0.20 mol), then the mixture was transferred into a 50 mL Teflon autoclave and sealed. After reacted at 230 °C for 5 days, a black solid was obtained and washed with water to remove undesired residuals. Note that the color of pure CuFeS_2 powder was brown. For convenience, we denoted the as-synthesized sample as $\text{CuFe}_{1-x}\text{Cr}_x\text{S}_2$ ($x = 0$,

0.1, 0.2, 0.3, 0.4). The chemical compositions were determined by atomic absorption spectra (see Table 1). The incorporated content of Cr^{3+} is not quantitatively the same but close to the initial loading ratio within experimental error. Attempts to synthesize pure $\text{CuFe}_{1-x}\text{Cr}_x\text{S}_2$ with $x = 0.5$ and 0.6 are failed, which, for instance, contain a substantial amount of CuCrS_2 .

Characterizations

Powder X-ray diffraction (XRD) was performed on a PANtical X'pert Pro diffractometer equipped with a PIXcel 1D detector and Cu $\text{K}\alpha$ radiation ($\lambda = 1.5406 \text{ \AA}$). Scanning electron microscope images were taken using a JEOL JSM-7800F electron microscope at a working distance of 4 mm. Transmission electron microscope images were recorded on JEM-2100F (accelerating voltage of 200 kV) equipped with Energy Dispersive X-ray Detector. Elemental analyses were performed with a flame atomic emission spectrometry. UV-Vis diffuse reflectance spectra were recorded on a Shimadzu UV-3600 spectrometer equipped with an integrating sphere attachment. BaSO_4 was used as a reflectance standard. The specific surface areas were determined by BET method with nitrogen adsorption at 77 K using a Quantachrome Quadrasorb SI analyzer. Prior to the measurements, samples were degassed at 180 °C for 5 h.

Photocatalytic evaluation

Photocatalytic activities were evaluated by photocatalytic reduction of nitrate ions under a 125W mercury light irradiation. The photocatalytic reactions were carried out in a cylindrical quartz photochemical reactor equipment with circulation water apparatus. In a typical run, 200 mL suspension containing nitrate ions (50 ppm N) and 50 mg solid catalyst ($\text{CuFe}_{1-x}\text{Cr}_x\text{S}_2$ or P25) was magnetically stirred in the dark to ensure the establishment of an adsorption-desorption equilibrium. Oxalic acid (0.005 mol/L) was used as the sacrificial agent.

Then, the reactor was exposed to a 125W mercury light for 1 hour. UV-Vis absorption spectrometry was applied to determine the residual contents of nitrate ions.

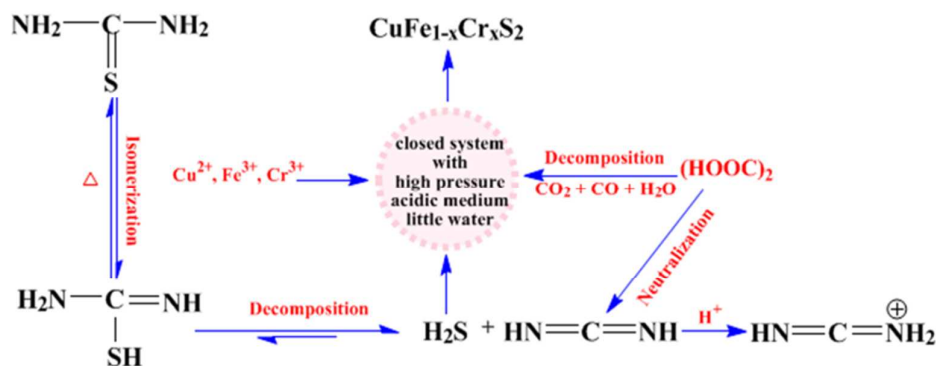
Results and discussion

Powder XRD patterns of as-prepared $\text{CuFe}_{1-x}\text{Cr}_x\text{S}_2$ ($x \leq 0.4$) are basically the same. The major phase matches well with the tetragonal chalcopyrite CuFeS_2 (see Fig. 2). Please note that the y-scale in Fig. 2 was presented as the intensity in square root. Several low-intensity peaks belonging to CuCrS_2 emerge when $0.2 \leq x \leq 0.4$ (The reference pattern of CuCrS_2 is also given in Fig. 2). We also attempted to prepare samples with higher Cr^{3+} concentrations, however, the samples initially loaded with the atomic ratio of $\text{Fe}^{3+}/\text{Cr}^{3+} = 0.5/0.5$ and $\text{Fe}^{3+}/\text{Cr}^{3+} = 0.4/0.6$ show a significant amount of CuCrS_2 . In other words, it is suggested that the upper limit of doping Cr^{3+} into CuFeS_2 is around 40 atom%, although with a small amount of CuCrS_2 impurity. The refined cell parameters, for $\text{CuFe}_{0.8}\text{Cr}_{0.2}\text{S}_2$ (as an example), are $a = 5.283 \text{ \AA}$ and $c = 10.420 \text{ \AA}$, almost the same with those of CuFeS_2 due to the similarity of cationic radii between Cr^{3+} and Fe^{3+} . All diffraction peaks are distinctly sharp, implying the high crystallinity.

SEM images for $\text{CuFe}_{0.7}\text{Cr}_{0.3}\text{S}_2$ sample were taken as shown Fig. 3. First, it suggests the homogeneity of the sample without any sign of amorphous component. And second, this sample is composed of micrometer particles which are in fact aggregations of nanometer crystallites. An element distribution analysis was performed on $\text{CuFe}_{0.8}\text{Cr}_{0.2}\text{S}_2$ sample by two-dimensional EDX mapping (see Fig. 4a) attached to a transmission electron microscope. It confirms the sub-micrometer morphology and the homogenous distribution of Cr^{3+} and Fe^{3+} all over the observed particle. The calculated atomic ration of Fe : Cr : S from EDX is close to the expected formula

$\text{CuFe}_{0.8}\text{Cr}_{0.2}\text{S}_2$. In addition, a selected area electron diffraction pattern was taken along the [001] direction (see Fig. 4b), which clearly shows a four-fold symmetry. The reflection conditions given in this ED pattern are $h + k = 2n$ for $hk0$ and $h = 2n$ for $h00$, which are expected for the space group $I-42d$.

During the usual hydrothermal synthetic condition, the ionization tendency of metal ions, especially Cr^{3+} , are quite high owing to high polarity of H_2O in aqueous medium, therefore it seems that random reactions of individual Cu^+ , Fe^{3+} or Cr^{3+} cation with S^{2-} are hardly avoidable.¹⁴ This is exactly why pure polymetallic sulfides (especially containing Cr^{3+}) are difficult to be synthesized using usual hydrothermal method.



Scheme 1. Possible mechanism for the formation of $\text{CuFe}_{1-x}\text{Cr}_x\text{S}_2$ in the thiourea-oxalic acid mixture system at 230 °C.

Here we experimentally obtained $\text{CuFe}_{1-x}\text{Cr}_x\text{S}_2$ by employing a co-molten solvothermal method, and we propose a possible mechanism for the synthetic process (See Scheme 1). Thiourea is an extensively used sulfurized reagent, and is unstable in near basic or neutral environments, which will slowly decompose into S^{2-} and $\text{H}_2\text{NC}\equiv\text{N}$ at about 150 °C.¹⁵ Thiourea will melt when heated at ~180 °C, then decompose by further elevating the temperature.¹⁶⁻¹⁸ For example, it was reported that thiourea starts to partially isomerize to ammonium thiocyanate (NH_4SCN) at temperature ranging

from 140 to 180 °C. Nevertheless, when thiourea was heated in either inert or air atmosphere at temperature between 182 and 240 °C, there are two directions for its decomposition, either form hydrogen sulfide together with carbodiimide ($\text{H}_2\text{S} + \text{HN}=\text{C}=\text{NH}$), or ammonia together with isothiocyanic acid ($\text{NH}_3 + \text{HNCS}$).¹⁹ The residual and molten thiourea serves as not only sulfurized reagent but also the solvent medium to facilitate the mass transfer.

When metal cations react with H_2S , the system will gradually become basic accompanied by the accumulation of carbodiimide or ammonia, which would eventually result in the formation of metal oxides. Then, oxalic acid is another key starting material, which melts at its melting point and starts to decompose into CO_2 , CO and H_2O at temperature above 189.5 °C. The residual oxalic acid and so-generated CO_2 probably behave as the acidic coupling reagents to neutralize the basic components ($\text{HN}=\text{C}=\text{NH}$ or NH_3) and accelerate the forward reaction (see Scheme 1). In the meantime, the gaseous components provide a high-pressure and slightly reductive environment, which can improve the crystallinity of the final products.

We tried several times to achieve higher Cr^{3+} concentrations (> 0.4), which resulted into a mixture of $\text{CuFe}_{1-x}\text{Cr}_x\text{S}_2$ and unwanted CuCrS_2 impurity (See Fig. 2). The co-molten method could facilitate the incorporation of Cr^{3+} into the chalcopyrite structure, but experimentally, it cannot produce a chalcopyrite-type “ CuCrS_2 ”, which apparently is not the thermodynamically stable phase, because there already exists a stable structure of CuCrS_2 with Cr^{3+} all in octahedral coordination. Here in our case, it is a competition to form a single phase of $\text{CuFe}_{1-x}\text{Cr}_x\text{S}_2$ or a mixture of chalcopyrite and CuCrS_2 . Our results shows the upper limit of Cr^{3+} into the chalcopyrite structure is around $x = 0.4$. Probably a more extreme condition would lead to a higher doping level.

As shown in Fig. 5a, UV–Vis reflectance spectra of $\text{CuFe}_{1-x}\text{Cr}_x\text{S}_2$ ($x = 0\sim 0.4$) solid solutions show

that all absorption bands are distributed from UV to the visible light region. Each absorption spectrum possesses an intense adsorption with a steep edge in the visible light region. And this steep edge indicates a band-gap transition of a semiconductor, not the $d-d$ transitions from transition metal cations.²⁰ The so-called optical energy gaps can be estimated using a classical Tauc approach.^{21, 22} Plots $(\alpha h\nu)^2$ against $h\nu$ based on the direct transition is shown in Fig. 5b, where α , h , ν , A , and E_g are absorption coefficient, Planck constant, light frequency, proportionality and band gap energy, respectively. The extrapolated value (the straight line to the x -axis) of $h\nu$ at $\alpha = 0$ gives the absorption edge energy corresponding to E_g . It is shown that the absorption edge energy decreases from 0.80 to 0.61 eV along with the increase of the Cr^{3+} concentration.

Catalytic reduction of nitrate ions is a new de-nitrification technology for drinking water, in which nitrate can be converted into innocuous N_2 over some specific catalysts.²³⁻²⁵ As shown in Fig. 6, we use commercial nanosize TiO_2 (P25) as a reference. The UV-light photocatalytic activity $((C_0-C)/C_0)$ of P25 is only 2% higher than the value from the blank photo-reduction experiment (without any catalyst). Apparently, $\text{CuFe}_{1-x}\text{Cr}_x\text{S}_2$ shows much high activities and we observe a linear enhancement along with the Cr^{3+} concentration up to $x = 0.4$. We also performed the photocatalytic experiments for the composite products with $x = 0.5$ and 0.6 . As shown in Fig. 6, there is a slight decrease of the photo-reduction percentage, which may due to the decrease of the active component $\text{CuFe}_{1-x}\text{Cr}_x\text{S}_2$. Anyway, Cr^{3+} -doped CuFeS_2 catalysts show significant high activities for the reduction of NO_3^- . In this work, it is found that $\text{CuFe}_{1-x}\text{Cr}_x\text{S}_2$ solid solutions have variable bandgap energies by rational substitutions of Cr^{3+} . The possible reason is that the narrowing of the band gap for $\text{CuFe}_{1-x}\text{Cr}_x\text{S}_2$ comparing to CuFeS_2 allow a higher absorption efficiency of photons.

Conclusions

$\text{CuFe}_{1-x}\text{Cr}_x\text{S}_2$ ($x \leq 0.4$) solid solutions have been successfully synthesized *via* a thiourea-oxalic acid co-molten solvothermal method. Oxalic acid plays an important role in the crystallinity of $\text{CuFe}_{1-x}\text{Cr}_x\text{S}_2$ and can greatly restrain the formation of other undesired impurities. The bandgap of $\text{CuFe}_{1-x}\text{Cr}_x\text{S}_2$ decreases monotonically as x increases, and importantly, by such a rational modification, we observe a predominant photocatalytic efficiency for nitrate ions reduction. A massive amount of Cr^{3+} is successfully incorporated into the chalcopyrite structure, comparing to the previous report $\text{CuGa}_{0.98}\text{Cr}_{0.02}\text{S}_2$. It is believed that this one-step and facile synthetic route is not only useful for synthesizing Fe^{3+} - Cr^{3+} solid solutions but also effective for other chalcopyrite systems, which offers opportunities to discover new photocatalysts.

Acknowledgements

This work was financially supported by the Nature Science Foundation of China (Grants 91222106, 21101175, 21171178, 21201012) and Natural Science Foundation Project of Chongqing (CSTC 2012jjA0438, 2014jcyjA50036). We also acknowledge the support from the sharing fund of large-scale equipment of Chongqing University.

References

- (1) N. Tsujii, T. Mori. *Appl. Phys. Express*, 2013, **6**, 043001.
- (2) M. Fujisawa, S. Suga, T. Mizokawa, A. Fujimori, K. Sato, *Phys. Rev. B*, 1994, **49**, 7155-7164.
- (3) D. Liang, R. Ma, S. Jiao, G. Pang, S. Feng, *Nanoscale*, 2012, **4**, 6265-6268.

- (4) N. Meng, B. Chris, V. Jagadese, *J. Am. Chem. Soc.*, 2006, **128**, 7118-7119.
- (5) G. Zhu, Z. Xu, *J. Am. Chem. Soc.*, 2009, **131**, 5691-5697.
- (6) I. Tsuji, H. Kato, H. Kobayashi, A. Kudo, *J. Am. Chem. Soc.*, 2004, **126**, 13406-13413.
- (7) F. M. R. Engelsman, G. A. Wiegers, F. Jellinek, B. Van Laar, *J. Solid State Chem.*, 1973, **6**, 574-582.
- (8) P. Chen, M. S. Qin, H. J. Chen, C. Y. Yang, Y. M. Wang, F. Q. Huang, *Phys. States Solidi A*, 2013, **210**, 1098-1102.
- (9) T. Watanabe, I. Nakada, *Jpn. J. Appl. Phys.*, 1978, **17**, 1745-1754.
- (10) Y. Wang, N. Bao, A. Gupta, *Solid State Sci.*, 2010, **12**, 387-390.
- (11) K. Chen, C. Chiang, D. Ray, *Mater. Lett.*, 2013, **95**, 172-174.
- (12) M. Wang, L. Wang, G. Yue, X. Wang, P. Yan, D. Peng, *Mater. Chem. Phys.*, 2009, **115**, 147-150.
- (13) J. Hu, Q. Lu, B. Deng, K. Tang, Y. Qian, Y. Li, *Inorg. Chem. Commun.*, 1999, **2**, 569-571.
- (14) A. Bhirud, N. Chaudhari, L. Nikam, R. Sonawane, K. Patil, J. Baeg, B. Kale, *Int. J. Hydrogen Energy*, 2011, **36**, 11628-11639.
- (15) S. Serge, S. Reuben, M. Sergei, *J. Phys. Chem. B*, 2001, **105**, 12634-12643.
- (16) S. Wang, Q. Gao, J. Wang, *J. Phys. Chem. B*, 2005, **109**, 17281-17289.
- (17) L. Stradella, M. Argentero, *Thermochim. Acta*, 1993, **219**, 315-323.
- (18) J. Madarász, G. Pokol, *J. Therm. Anal. Calorim.*, 2007, **88**, 329-336.
- (19) Z. Wang, M. Yoshida, B. George, *Comput. Theor. Chem.*, 2013, **1017**, 91-98.
- (20) D. Jing, L. Guo, *J. Phys. Chem. B*, 2006, **110**, 11139-11145.
- (21) D. Wang, T. Kako, J. Ye, *J. Am. Chem. Soc.*, 2008, **130**, 2724-2725.

- (22)A. Ishikawa, T. Takata, J. Kondo, M. Hara, H. Kobayashi, K. Domen, *J. Am. Chem. Soc.*, 2002, **124**, 13547-13553.
- (23)S. Jacinto, J. Montero, D. Elizabeth, J. A. Aderson, *Appl. Catal., B: Environ.*, 2007, **73**, 98-105.
- (24)N. Barrabés, A. Dafinov, F. Medina, J. E. Sueiras, *Catal. Today*, 2010, **149**, 341-347.
- (25)K. Doudrick, T. Yang, K. Hristovski, P. Westerhoff, *Appl. Catal., B: Environ.*, 2013, **136**, 40-47.

Table 1. BET surface and chemical compositions of $\text{CuFe}_{1-x}\text{Cr}_x\text{S}_2$.

Expected molecular formula	Initial loading ratio	Ratios from AAS	BET surface
	Molar ratio (Cu/Fe/Cr)	Molar ratio (Cu/Fe/Cr)	(m^2/g)
CuFeS_2	1/1/0	1/0.78/0.01	9.0
$\text{CuFe}_{0.9}\text{Cr}_{0.1}\text{S}_2$	1/0.9/0.1	1/0.77/0.06	10.3
$\text{CuFe}_{0.8}\text{Cr}_{0.2}\text{S}_2$	1/0.8/0.2	1/0.75/0.20	8.0
$\text{CuFe}_{0.7}\text{Cr}_{0.3}\text{S}_2$	1/0.7/0.3	1/0.68/0.31	11.0
$\text{CuFe}_{0.6}\text{Cr}_{0.4}\text{S}_2$	1/0.6/0.4	1/0.58/0.41	15.3

Figures

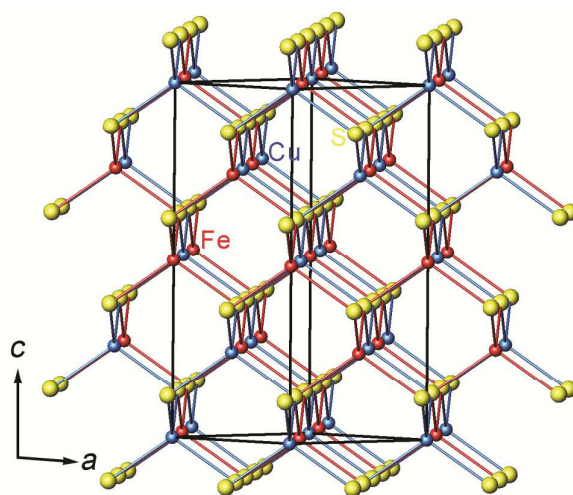


Fig. 1. A structure view of chalcopyrite CuFeS_2 . Blue, red and yellow spheres represent Cu, Fe, S, respectively. Cu^+ and Fe^{3+} are both tetrahedrally coordinated by S^{2-} .

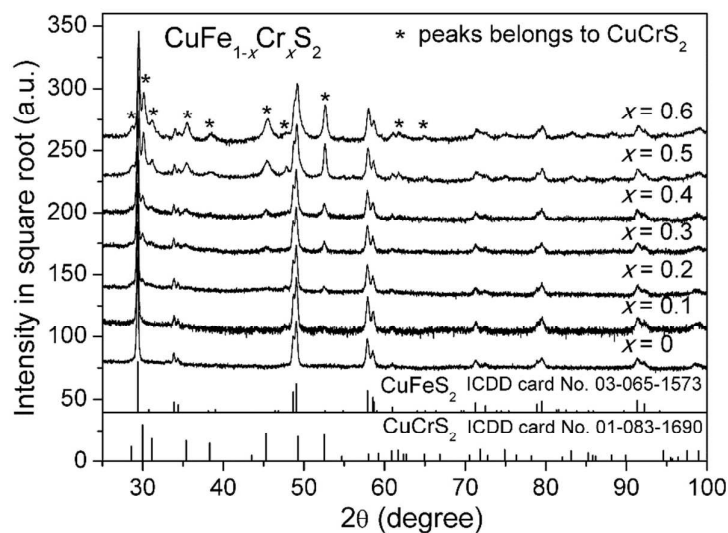


Fig. 2. XRD patterns of $\text{CuFe}_{1-x}\text{Cr}_x\text{S}_2$ solid solutions prepared by co-molten solvothermal method. Only tiny impurities were observed for $0.2 \leq x \leq 0.4$, while there are obvious impurity peaks from CuCrS_2 when $x = 0.5$ and 0.6 . The reference patterns for CuFeS_2 and CuCrS_2 are given at the bottom. Note that the y-scale is presented as the square root of the intensity.

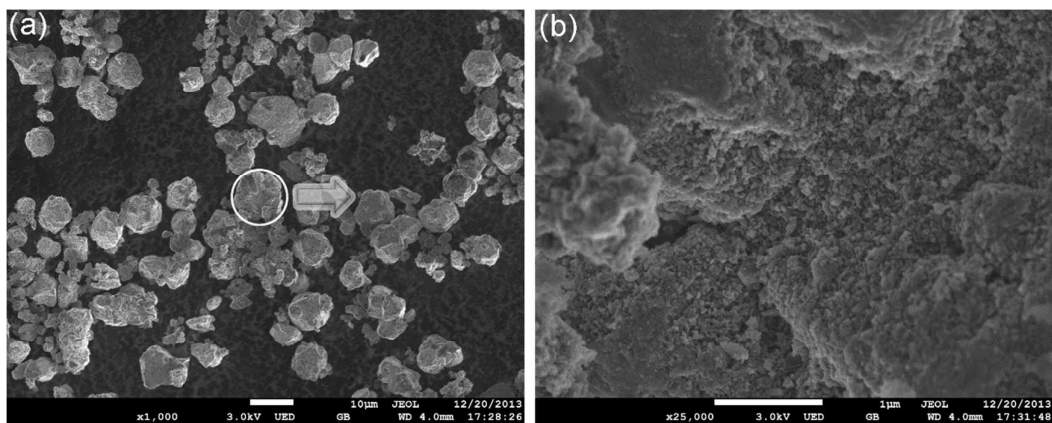


Fig. 3. SEM images taken by JSM-7800F for $\text{CuFe}_{0.7}\text{Cr}_{0.3}\text{S}_2$ sample.

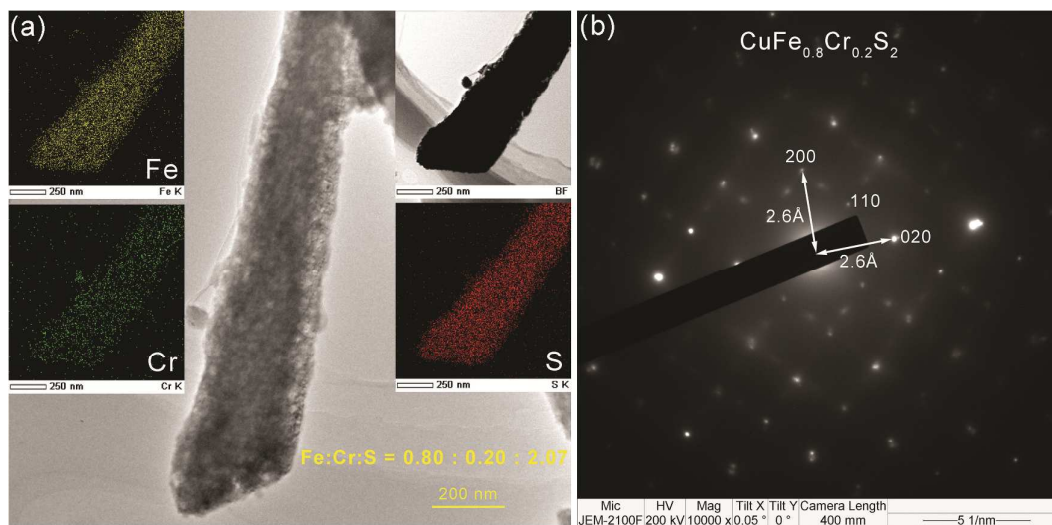


Fig. 4 (a) TEM image for CuFe_{0.8}Cr_{0.2}S₂ as a representative. The inserts are elemental distributions of Fe, Cr, and S; (b) a selected area electron diffraction pattern along the [001] direction.

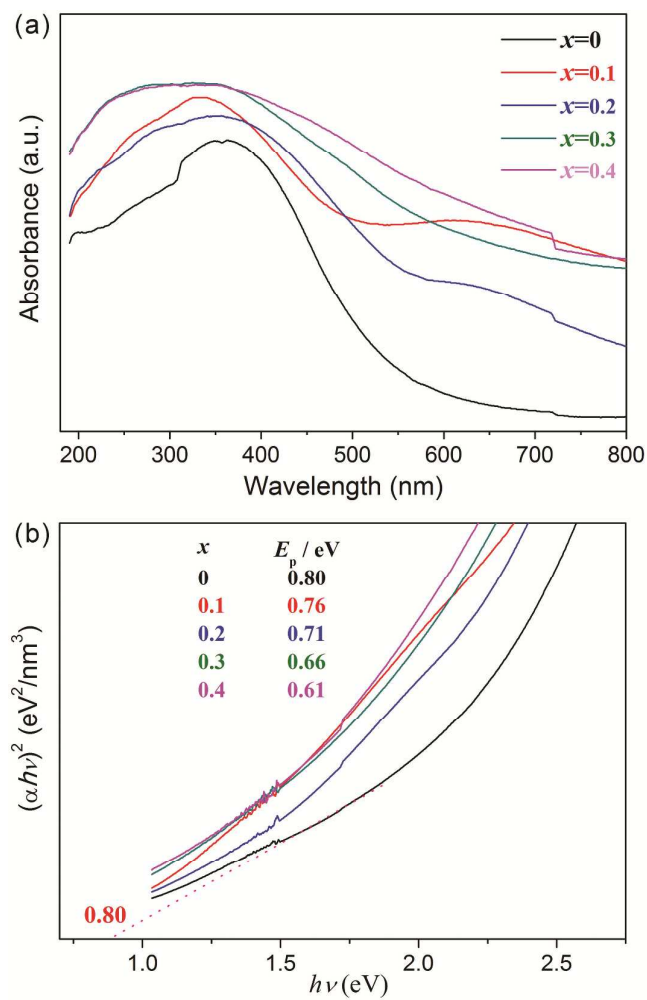


Fig. 5. (a) UV-Vis diffused reflectance spectra of CuFe_{1-x}Cr_xS₂ solid solutions; (b) calculated band gap energy E_g with plots of $(\alpha h\nu)^2$ against photo energy ($h\nu$).

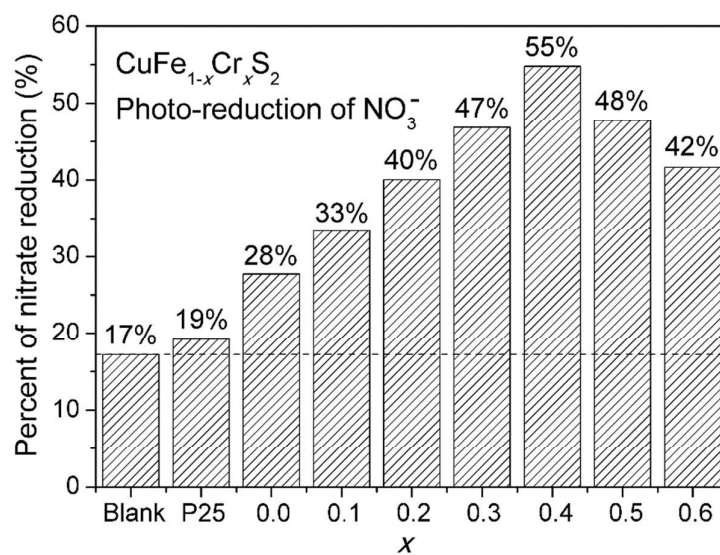


Fig. 6. Photocatalytic reduction of nitrate using CuFe_{1-x}Cr_xS₂ catalysts with different contents of Cr³⁺ (1 hour irradiation).